

dominated by a three-stranded antiparallel  $\beta$  sheet that includes 60% of all residues (20–24). The molecule appears sufficiently rigid that the crystal structure must provide a good model both for the conformation in solution and at the site of action. The constraints of the three disulfide bonds prohibit a gross conformational change, such as that proposed for colicin A (25), upon moving from an aqueous to an apolar milieu. This appearance of stability is supported by the similarity of the two molecules in the asymmetric unit. All main-chain atoms of the two molecules superpose with a root-mean-square (rms) deviation of 0.82 Å. The only significant departure from noncrystallographic symmetry is an apparent flexing motion of residues 20 to 25. If these residues are omitted from the least squares superposition, the deviation of main-chain atoms of the two monomers becomes 0.32 Å.

The pattern of conserved residues of the defensin family (Fig. 2) can be interpreted in terms of the three-dimensional structure and suggests that all other defensins have conformations similar to HNP-3. The six Cys residues that must play a major role in stabilizing the conformation are invariant. Moreover, several other key structural residues, Arg<sup>6</sup>, Glu<sup>14</sup>, and Gly<sup>24</sup>, are found in every defensin except GPNP. Gly<sup>24</sup> occupies the third position of a type I' turn; Arg<sup>6</sup> forms a salt bridge with Glu<sup>14</sup> that spans the only stretch of polypeptide that does not participate in the  $\beta$  sheet (26). Nuclear magnetic resonance (NMR) studies of NP-5 (27–29) also support the view that all known defensin sequences can fold as HNP-3.

HNP-3 crystallizes as a dimer. The two molecules in the asymmetric unit are in close contact and are related to each other by a local twofold rotation axis. The three-stranded  $\beta$  sheet of the monomer is extended across this interface to form a six-stranded sheet in the dimer. Figure 1B shows how four hydrogen bonds link the two monomer sheets directly and that two more hydrogen bonds extend the intermolecular  $\beta$ -sheet interaction through well-ordered water molecules. The dimeric association is further stabilized by hydrophobic interactions, especially between Cys<sup>5</sup>, Cys<sup>20</sup>, Tyr<sup>22</sup>, and Phe<sup>28</sup> from each of the monomers. Equilibrium centrifugation confirmed that HNP-3 is a dimer or higher polymer in solution under conditions identical to the crystallization conditions but without the PEG 8000 (30). The presence of the invariant Gly<sup>18</sup> at the dimer interface also suggests that defensin is a dimer at the site of action. If Gly<sup>18</sup> were replaced by any other residue, the C $\beta$  atom would overlap with the O atom of residue 20 from the neighboring monomer.

The observed dimeric association suggests several hypotheses for the killing mechanism of defensins, as discussed below.

The shape of the dimer resembles a basket with an apolar base and a polar top that includes the two amino termini and the two carboxyl termini (Figs. 1C and 3A). The  $\beta$  sheet both twists and coils, and as a result the amino-terminal  $\beta$  strands of the two neighboring monomers are close together in space (Fig. 1C). These two  $\beta$  strands are hydrogen-bonded together through ordered

solvent molecules that form a mini-channel, which passes right through the dimer (Fig. 1, D and E). The core of this basket is hydrophobic and, at the center of the dimer interface, the disulfide bonds between residues 5 and 20 of the two molecules are in van der Waals contact with each other. Six Arg residues form an equatorial ring around the dimer; these side chains are relatively flexible and three of them cannot be located in Fourier maps.

The dimeric crystal structure suggests

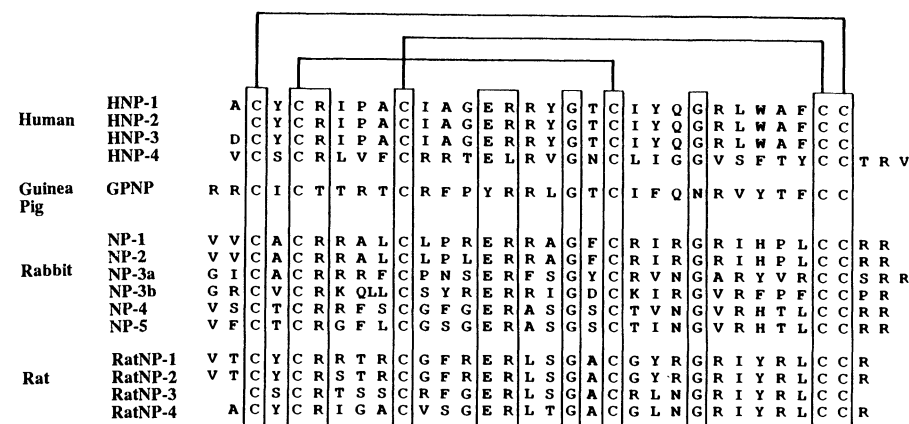


**Fig. 2.** The amino acid sequences of HNP-3 and other defensins (39, 40) are referred to a common numbering scheme. As a result the 30-residue HNP-3 starts with residue number 2 and ends with residue number 31. The disulfide connectivity is indicated and residues are boxed if conserved in at least all but one of the sequences.

**Table 1.** Data collection and structure determination. HNP-3 was purified as described (34), and crystals were grown at room temperature in 4- $\mu$ l hanging drops. The drop consisted of a 50:50 mixture of reservoir and 20 mg ml<sup>-1</sup> protein in 0.01% acetic acid, the reservoir solution was 15% PEG 8000, 10% isopropanol, 100 mM sodium citrate at pH 4.0. Crystals would usually grow in about 4 days and were harvested into the reservoir solution without loss of diffraction properties. The space group is  $P2_12_12$  with  $a = 30.8$  Å,  $b = 45.0$  Å, and  $c = 40.3$  Å. There are two defensin monomers in the asymmetric unit, and the crystal contains 38% solvent. These HNP-3 crystals are apparently isomorphous to one of the forms reported for the closely related HNP-1 (35). A total of six derivatives were identified by locating the heavy-atom positions by using Patterson and Fourier methods. Inspection of several Fourier maps showed density that clearly corresponded to a Trp side chain. Once this feature had been recognized, many maps calculated with the use of different combinations of derivatives, with and without solvent flattening (36), were assayed by the quality of this Trp density. The best map was that calculated from  $K_2Pt(CN)_4$  (20 mM, 24-hour soak, three sites) and  $Pt(NH_2)_2(NO_2)_2Cl_2$  derivatives (13 mM, 4.5-day soak, one site) after solvent flattening. Maps phased on both of these derivatives but before solvent leveling, or based on just the  $K_2Pt(CN)_4$  derivative after solvent flattening, were also of high quality. The mean figure of merit after solvent flattening was 0.73. These three maps were displayed on an Evans and Sutherland PS390, and an atomic model was easily fitted with the program FRODO (37).

Parameter	Native	$K_2Pt(CN)_4$	$Pt(NH_2)_2(NO_2)_2Cl_2$
$R_{iso}^*$		0.16	0.11
Resolution limit ( $d_{min}$ , Å)	1.9	2.4	2.5
Observations (no.)	22,975	18,559	16,019
Rejected during processing (no.)	1,617	179	850
Unique reflections (no.)	4,524	2,390	2,128
% Complete	(95.9)	(99.5)	(99.4)
$ F  > 2\sigma_F$ (%)	96.7	97.7	98.9
$R_{sym}^\dagger$	0.054	0.048	0.057
Rms $F_h/E\ddagger$ (centrics)		1.38	0.70
Rms $F_h/E$ (acentrics)		1.57	0.94
$R_{Cullis}^\S$		0.53	0.70

\* $R_{iso} = (\sum |F_{derivative}| - |F_{native}|) / \sum |F_{native}|$ .  $\dagger R_{sym} = (\sum |I_i| - |I_{av}|) / \sum |I_{av}|$ ; this value is calculated before rejecting any observations.  $\ddagger F_h$  is the heavy-atom structure factor and  $E$  is the residual lack of closure.  $\S R_{Cullis} = (\sum |F_{h(obs)}| - |F_{h(calc)}|) / \sum |F_{h(obs)}|$ .